Characterization of precipitation and recharge in the peripheral aquifer of the Salar de Atacama

Sonia Valdivielso [a,b,*], Enric Vázquez-Suñé [a], Christian Herrera [c], Emilio Custodio [d,e,f]

[a] *Institute of Environmental Assessment and Water Research (IDAEA/CSIC), C/Jordi Girona 18-26, 08034 Barcelona, Spain*
[b] *University of Barcelona (UB), C/Martí i Franquès, 08028 Barcelona, Spain*
[c] *Centro de Investigación y Desarrollo de Ecosistemas Hídricos, Universidad Bernardo O'Higgins, Santiago, Chile*
[d] *Groundwater Hydrology Group, Department of Geo-Engineering, Technical University of Catalonia (UPC), C/Jordi Girona 1-3, 08034 Barcelona, Spain*
[e] *Royal Academy of Mathematical, Physical and Natural Sciences (RAC) of Spain*
[f] *Instituto de Estudios Ambientales y Recursos Naturales (iUNAT), Universidad de Las Palmas de Gran Canaria, Islas Canarias, Spain*

HIGHLIGHTS

- In summer, the air comes from the North and South Atlantic and the Pacific Ocean.
- In winter, all the air masses come from the Pacific Ocean.
- Precipitation is more depleted in heavy isotopes in winter than in summer.
- Recharge to peripheral aquifers originates within the hydrological basin.

GRAPHICAL ABSTRACT
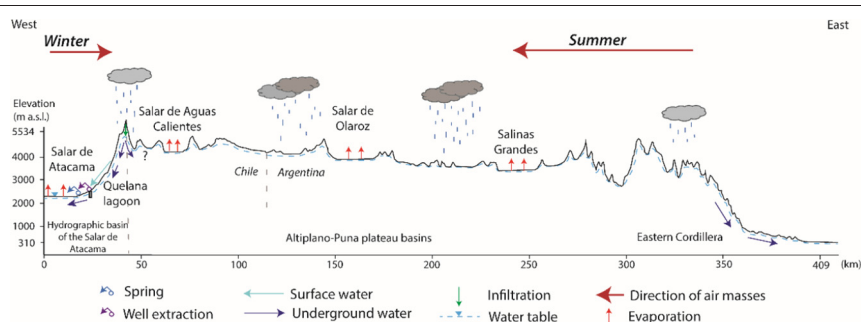
ARTICLE INFO

ABSTRACT

To reduce uncertainty in the identification of the recharge areas in the Peripheral Aquifer of the Salar de Atacama (SdA), a few studies have investigated the isotopic characteristics and moisture sources of precipitation in the SdA basin. In the present study, the seasonal cycle of meteorological parameters and the relationships of this cycle with sea surface temperature anomalies are shown, the sources of humidity are identified, and the types of clouds producing precipitation are defined. Finally, the isotopic compositions of precipitation, surface water and groundwater in the SdA basin and the Altiplano-Puna Plateau basins are analysed to identify the area recharging the northern, eastern and southern subbasins of the SdA. In summer, when the highest temperature, relative humidity and precipitation values of the year are recorded, the precipitation is due to deep convection. The trajectories of the arriving air masses can be classified into three groups: from the North Atlantic Ocean across the Amazon basin, from the South Atlantic Ocean across the La Plata River basin and the Gran Chaco, and from the Pacific Ocean. In winter, when the temperature, relative humidity and precipitation are lower, the moisture masses come from the Pacific Ocean. Winter precipitation is more depleted in heavy isotopes than summer precipitation. The isotopic analysis of precipitation, surface water and groundwater shows that recharge of the eastern subbasins of the SdA occurs by diffuse infiltration of precipitation and concentrated infiltration of surface water, both within the hydrographic basin of the SdA. The meteoric source of the waters in the Altiplano-Puna Plateau basins is isotopically lighter than the waters found in the side basins of the SdA, so there is no significant water quantity transfer to the peripheral aquifers of the SdA from outside the hydrographic basin.

---

* Corresponding author at: Institute of Environmental Assessment and Water Research (IDAEA/CSIC), C/Jordi Girona 18-26, 08034 Barcelona, Spain.
E-mail address: sonia.valdivi@gmail.com (S. Valdivielso).

1. Introduction

The basin of the Salar de Atacama has a flourishing tourist activity, some of the most important mining activity in Chile to extract brines for lithium production, protected lagoon ecosystems, and local livestock, which require sufficient and secure water resources (Marazuela et al., 2018; Munk et al., 2021). For this reason, it is necessary to quantify the water budget in as much detail as possible. Therefore, the first step to facilitate environmentally and economically viable long-term management is a good understanding of the source and location of recharge of the aquifers along the periphery of the Salar de Atacama. Despite the efforts of the General Water Directorate of Chile (DGA) and mining companies through numerous technical studies (CORFO - Amphos 21, 2018; DGA, 1986, 2013; GCF Ingenieros - DGA, 2010; IDAEA-CSIC, 2017) and the results developed in related scientific papers, two hypotheses exist regarding the recharge mechanisms and rates of the Salar de Atacama peripheral aquifers (Fig. 2). Distinguishing between these two hypotheses is of paramount importance for understanding the water balance. One of the hypotheses assumes that groundwater recharge occurs from the Altiplano-Puna Plateau basins to the Salar de Atacama (Boutt et al., 2016, 2021; Corenthal et al., 2016; Moran et al., 2019; Salas et al., 2010). The other hypothesis assumes that the recharge area is entirely inside the hydrographic basin of the Salar de Atacama basin (DGA, 2013; IDAEA-CSIC, 2017; Marazuela et al., 2019a, 2019b, 2018, 2020).

The elevation of recharge sites have been estimated with the water stable isotope (δ^{18}O and δ^{2}H) composition data in dozens of areas around the globe (Jasechko, 2019). This estimation is possible because the oxygen and deuterium isotopic compositions of precipitation water are not changed once infiltration converts to in-transit recharge for the aquifer, so their values at any point in the aquifer reflect the isotopic conditions of the recharge zone (RAEMIA, 2019). Therefore, once the isotopic contents of precipitation are spatially and temporally characterized, the recharge source of the aquifers of the different geomorphological units in northern Chile can be determined. Due to the low and irregular rainfall in arid zones, which are primarily short, sporadic events, it is difficult to monitor the chemical and isotopic compositions of rainwater. Research in these areas needs several years until sufficient data on rain are collected to characterize its chemical and isotopic compositions in different locations. Diverse studies have dealt with the origin of groundwater through isotopic analysis in the Antofagasta region. Each study has taken a different approach. Cortecci et al. (2005) focused on the El Tatio geothermal field. CRICYT (2017) identified the water source used by the *algarrobos* (corib trees) of the Salar de Atacama. Godfrey et al. (2003) identified the meteoric water source for the Salar de Atacama and Altiplano basins considering paleoclimate effects. Herrera et al. (2016) considered the connection between highland basins. Lagos (2016) studied the sources of the hot springs. Moran et al. (2019) studied the sources feeding discharges in the Salar de Atacama.

The objectives of this research are (1) to find the origin of the air masses that cause precipitation, (2) to identify the type of clouds, (3) to characterize the isotopic composition of precipitation producing recharge and (4) to identify the recharge areas of the northern, eastern and south-eastern subbasins of the Salar de Atacama based on isotope composition.

The cases that are considered here correspond to the northern, eastern and south-eastern peripheral subbasins of the Salar de Atacama and the basins at the Altiplano-Puna Plateau in northern Chile (Fig. 1). The western half of the Salar de Atacama basin is not studied, as it contributes less than 1% of the recharge to the peripheral aquifers of the salt flat (IDAEA-CSIC, 2017; Munk et al., 2018). Deep groundwater inflow below the halite salt nucleus (core) is not considered in this investigation. Its possibility was suggested by Marazuela et al. (2020) and Munk et al. (2018, 2021).

2. Study area

The Salar de Atacama (Figs. 1 and 2) is the largest salt deposit in Chile and the third largest in America. It is approximately 100 km long and 80 km wide, covering an area of approximately 3100 km^2 (IDAEA-CSIC, 2017). It contains 40% of the world reserves of lithium and large amounts of boron and potassium salts. The elevation of the Salar de Atacama is 2300 m above sea level (m asl) (Tejeda et al., 2003). The central depression is occupied by a nucleus (core) composed essentially of 1100 km^2 of halite, 900 m thick, surrounded by a marginal zone of saline silt flats with a surface area of approximately 2000 km^2 (IDAEA-CSIC, 2017). The nucleus contains interstitial sodium chloride brine, which is rich in magnesium, potassium, lithium and boron.

The Salar de Atacama basin is an endorheic area located in a tectonic depression filled by clastic and evaporitic sediments. It covers an area of approximately 13,300 km^2 (Mardones, 1998) and it is bounded to the west by the Cordillera de la Sal, which extends from NNE to SSW on the slopes of the Cordillera de Domeyko and to the east by the Cordillera Occidental of the Andes (Andean Western Range). There are high peaks that correspond to active volcanic arc edifices (>5500 m asl). Other limits are the El Tatio Mountains to the north and the Cordón de Lila mountains and Sierra de Varas to the south (Figs. 1 and 2) (Rubilar et al., 2018; Tejeda et al., 2003).

The annual mean temperature and precipitation rate in the Salar de Atacama basin are 14 °C and 160 mm/year, respectively (Risacher et al., 1998). During the austral summer (December-March), the greatest amount of annual rainfall (87% of annual rainfall) occurs, due to the intensification of the easterly winds that carry masses of humid air (Fuenzalida and Rutllant, 1986) that come from the Atlantic Ocean and cross the Amazon basin (Garreaud et al., 2003; Garreaud, 1999, 2000; Vuille, 1999) and the Gran Chaco (Dapeña and Panarello, 2005; González et al., 2009; Valdivielso et al., 2020). This intensification of the easterly winds causes masses of humid air to cross to the west and generate precipitation in the study area. During the austral winter (June-September), the Pacific anticyclone approaches the coast and cold ocean currents come from the Antarctic (i.e., the Humboldt Current) (Aravena et al., 1999; Sánchez-Murillo et al., 2018; Vuille et al., 1998). The winds from the Pacific Ocean carry dry air masses towards the interior of the continent, thus producing little precipitation, amounting about 7% of annual rainfall (Garreaud et al., 2003; Pourrut and Covarrubias, 1995; Vuille, 1999; Vuille and Ammann, 1997). During some wet winters, numerous snowfalls occur in the study area (Houston, 2006a; Saavedra et al., 2017, 2018; Vuille, 1999; Vuille and Baumgartner, 1998).

The Salar de Atacama basin contains the Rio Grande River and its tributaries, the San Pedro River and the Vilama River, which flow from north to south towards the salt flat (Salas et al., 2010). There are also some intermittent streams (brooks, *quebradas*) descending from the Andes mountain range, whose water from storm runoff and springs infiltrates in the extensive alluvial fans on the east side of the Salar. There are lagoon systems and associated ecosystems belonging to the Los Flamencos National Reserve in Soncor, in the northern Salar de Atacama. Since 1996, the Soncor lagoons have been included in the Ramsar Convention's international list of wetlands. The springs at the northern freshwater-saline water mixing zone and the Soncor lagoons are related to structural controls (faults and fractures) (Marazuela et al., 2018).

The Salar de Atacama is the current depocentre of an endorheic basin where a series of clastic, volcanic and evaporitic sediments have been deposited from the Upper Cretaceous to the present (IDAEA-CSIC, 2017). The basement of the Salar de Atacama is gently folded and strongly faulted. It is formed by lavas from the Upper Miocene to the Holocene, ignimbrites from the Upper Miocene to the Pleistocene, and red sediments from the Paleozoic belonging to the Peine and Cas Formations (Ramírez and Gardeweg, 1982; SERNAGEOMIN, 2003). The erosive surface of the basement is covered by the ignimbrite deposits. The alluvial
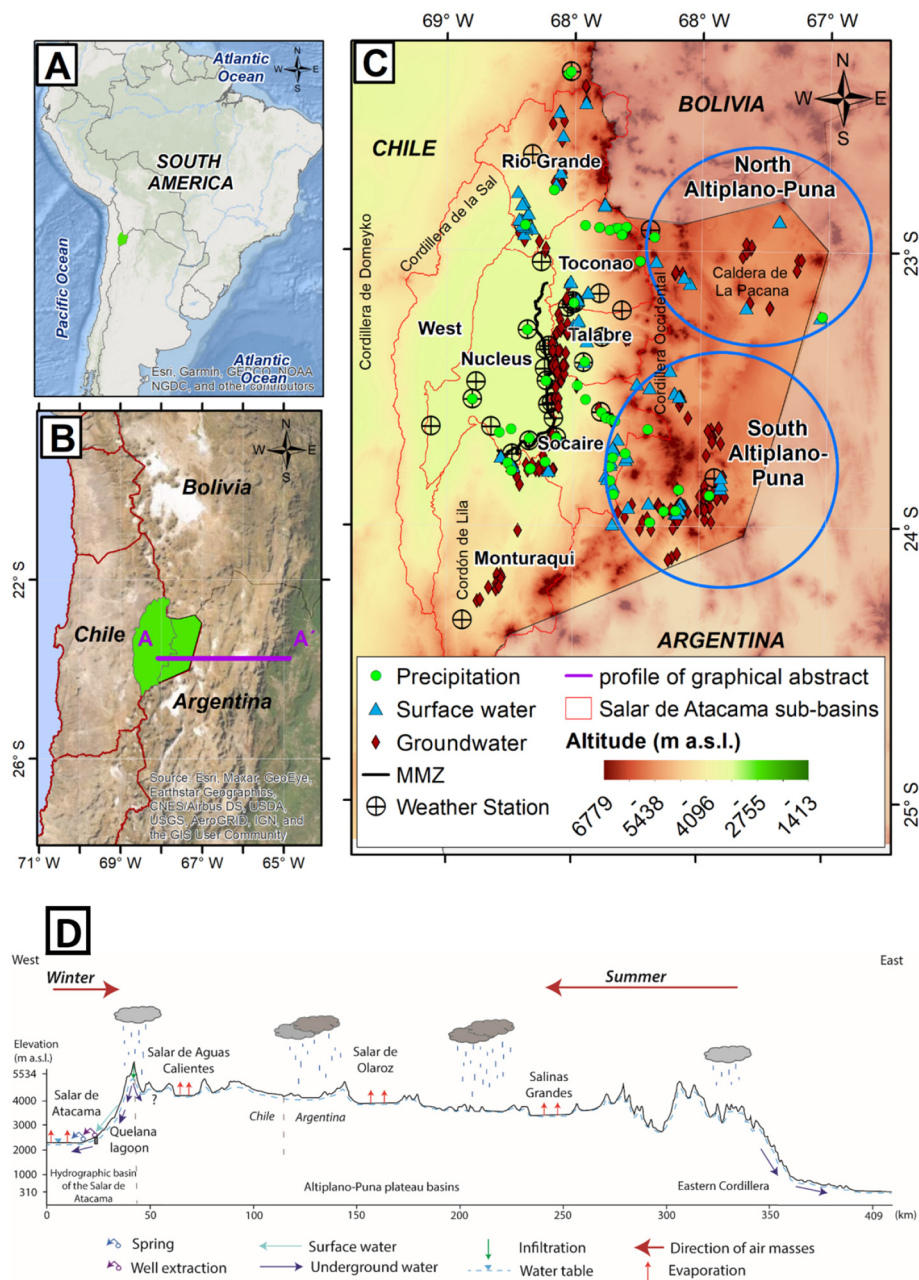
Fig. 1. Location map of the study area. A) Location in South America. B) The green area is the Salar de Atacama and basins in the Altiplano–Puna plateau in the Antofagasta region (northern Chile) (base map from satellite data SRTM. http://earthexplorer.usgs.gov/). C) Boundaries of the sub-basins of the Salar de Atacama and location of water samples; the black line is the Middle Mixing Zone (MMZ) in the Salar de Atacama defined by Marazuela et al. (2018) and the blue circles in the Altiplano–Puna indicate the plateau zones. D) Profile West-East (A-A′) of studied area with indication of the assumed water table.

deposits are made up of Quaternary detrital materials. On the eastern side of the Salar de Atacama, the ignimbrites and alluvial fans constitute an important hydrogeological and geomorphological transition zone between the volcanic chains and the depression containing the salt flat. The numerous ignimbrite layers and alluvial fans constitute important controls on springs and diffuse flows (intermittent streams) at the margin of the basin floor (Jordan et al., 2002). Often, nonwelded and moderately welded fractured ignimbrites have high water infiltration capacity (Marazuela et al., 2019a) and, when they are below the water table, they may constitute local and regional aquifers. The welded ignimbrites may act as confining units (Herrera et al., 2016). The large alluvial fans along the margins of the Salar provide substantial groundwater storage capacity and allow flow in the lower eastern slopes (Houston, 2009).

To the east of the Salar de Atacama, there is the Altiplano - Puna Plateau, whose altitude is greater than 4000 m asl. It contains small endorheic basins limited by Upper Miocene to Holocene volcanoes and covered by Quaternary alluvial fan deposits in its lower parts. Usually, these basins have lagoons, such as the Miscanti and Miñique lagoons, or salt flats in their lower parts, such as Tara, Pujsa and Aguas Calientes, in the basins of the Altiplano-Puna Plateau. The basins of the north-eastern Altiplano-Puna Plateau are larger and formed by Paleozoic rocks and Palaeogene alluvial sedimentary rocks (SERNAGEOMIN, 2003). Several studies have investigated recharge to the aquifers of some of these basins in the southern part of the Altiplano-Puna Plateau inside the large volcanic-tectonic Caldera de La Pacana and the extension to the south (Herrera et al., 2016, 2019; Urrutia et al., 2019).
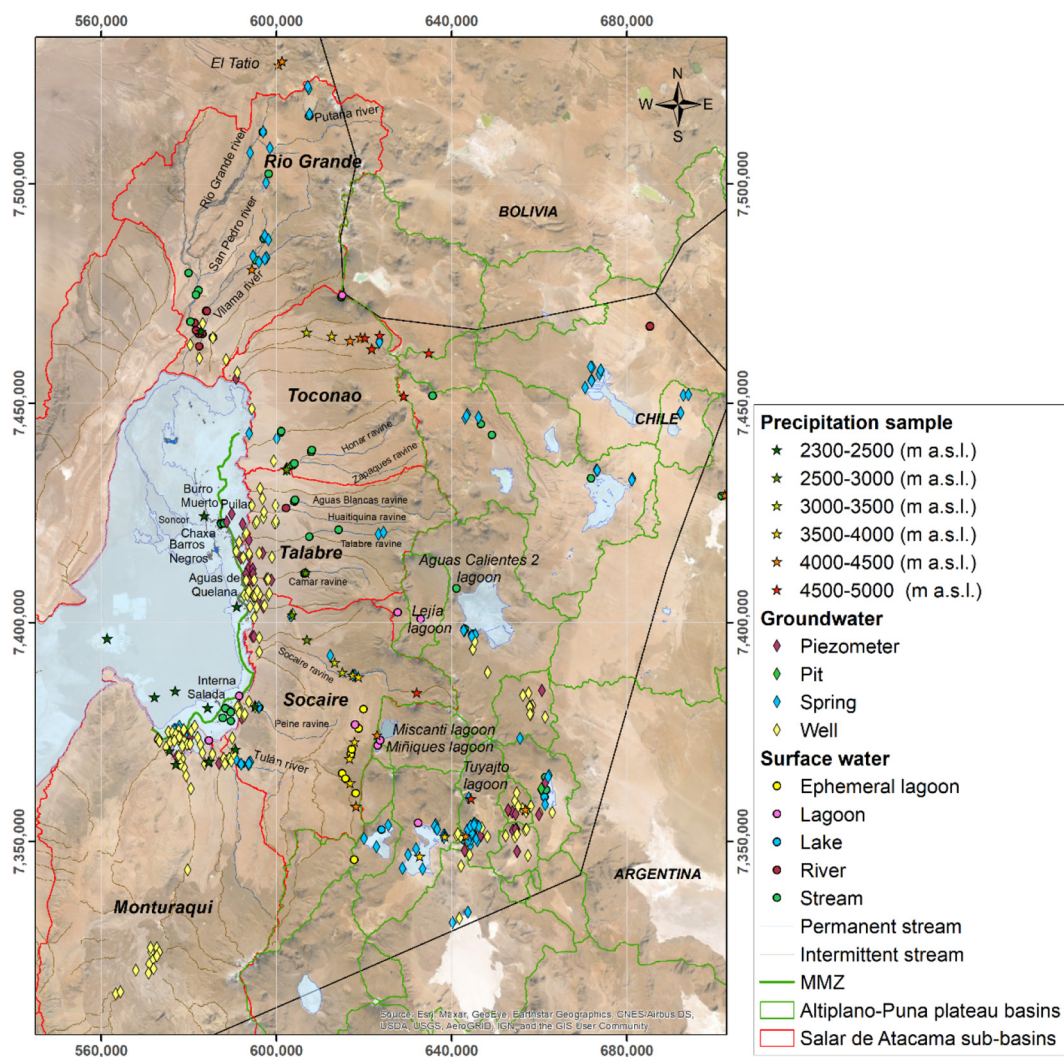
Fig. 2. Location map of water samples with isotopic analysis. The map includes the precipitation stations, the permanent streams, the intermittent streams, and the middle mixing zone (MMZ) in the peripheral aquifers to the Salar de Atacama.

Most of the studied water points are on the periphery of the Salar de Atacama. The surface water corresponds to lagoons, and the numerous groundwater samples correspond to study, monitoring and sampling boreholes and pits related to the Salar. However, in the slopes of the basin, surface water samples correspond to lakes/lagoons, springs, permanent streams (rivers) and intermittent surface water flows after rainfall events and snowmelt periods, and groundwater samples are scarce. The boreholes are used to obtain groundwater for mining activities in the Salar de Atacama and for investigations carried out in the Altiplano basins as part of the environmental impact studies needed to obtain mining concessions. The different points considered here, which include most of the existing ones, are shown in Figs. 1 and 2.

3. Material and methods

3.1. Meteorological data

This study uses daily meteorological data on atmospheric temperature, relative humidity and precipitation from 1973 to 2020 (Fig. 1). The records correspond to 31 automatic weather stations belonging to the General Directorate of Waters of Chile (Center for Climate and Resilience Research, 2020; DGA, 2020) and Soquimich (SQM) mining company. These 30 weather stations are located at elevations from 2300

to 4825 m asl, with 20 of them between 2300 and 2500 m asl, in the nucleus and the marginal zone of the Salar. The data used in this work are available as Supplementary Material (SM_Meteorological_data).

3.2. Back trajectory analysis

Back trajectory analysis is a commonly used method to identify atmospheric transport patterns and/or determine the origins and pathways of trace substances in the air (Cabello et al., 2008). Air mass back trajectory analyses were obtained using the Hybrid Single Particle Lagrangian Integrated Trajectory (HYSPLIT) Model v.4 (Draxler and Hess, 1997; Draxler, 1999; Stein et al., 2015), with meteorological datasets available from the Air Resources Laboratory (ARL) of the National Oceanic and Atmospheric Administration (NOAA, USA). Each trajectory was calculated using data from the National Centers for Environmental Prediction/National Center for Atmospheric Research (NCEP/NCAR) Global Reanalysis meteorological reanalysis pressure (RP) data files as input for the HYSPLIT model at 240 h' time steps back at 1500, 3000, 5500 m AGL (above ground level) for the coordinates of the Chaxa and LZA3-1 rain samplers on the days in which rain was recorded at the weather stations. Two-hundred forty hours was considered sufficient time to identify the time of arrival from the ocean to the collection point of the precipitation sample.

3.3. Outgoing longwave radiation

Non-interpolated outgoing longwave radiation (OLR) is a measure of the amount of energy emitted into space by the Earth's surface, oceans and atmosphere. OLR values are often used as a proxy for convection in subtropical-tropical regions, as maximum cloud temperatures are an indicator of cloud height: the lower the temperature is, the higher the clouds are (Liebmann, 1996; Morales et al., 2018; Risi et al., 2008a, 2008b; Vuille et al., 2008).

Non-interpolated daily OLR values from 2002 to present are taken from the twice daily Advanced Very High Resolution Radiometer (AVHRR) OLR soundings at 2.5° × 2.5° resolution provided by NOAA/OAR/ESRL PSL, Boulder, Colorado, USA (https://psl.noaa.gov/data/gridded/data.uninterp_OLR.html#detail) at the LZA3-1 and Chaxa sampling points.

3.4. Isotopic data

As shown in Fig. 2, the isotopic analysis dataset consists of three types of water that were collected in the study area: (1) precipitation, (2) surface water and (3) groundwater. As it is a large dataset, data were grouped by subbasins in the Salar de Atacama and Altiplano-Puna Plateau basins. To facilitate the discussion, it is convenient to distinguish between the northern subbasins (Salar de Aguas Calientes, Lejia lagoon, Miscanti and Miñique lagoons, Tuyajto lagoon, Salar de Laco, Salar de Talar, and Salar de Incaguasi) and the southern subbasins (Salar de Tara, Salar de Quisquiro (or Salar de Layaques), Salar de Pujsa, Parico lagoon, and Helada lagoon). Fig. 2 shows the most important locations. The datasets used in this work are available as Supplementary Material (SM_Isotopic_data).

In the study area, Eight passive precipitation samplers (submerged tube totalizers) were installed that allowed rain samples with practically no evaporation to be obtained, for subsequent analysis of stable isotopes in water, as required for global monitoring networks of the isotopic composition of precipitation (Antonio, 2018; dos Santos et al., 2019; Duvert et al., 2016; Esquivel-Hernández et al., 2019; Gröning et al., 2012). Some samples correspond to precipitation of a month or a few months, with many months in which there was no precipitation. The samplers were installed in the core of the salt flat in the village of Toconao, near the Chaxa, Quelana and Interna lagoons, in the El Tatio geothermal field (to the NE, outside Fig. 2), in the Atacama Large Millimeter/submillimeter Array (ALMA) observatory and at Paso Jama on the border between Chile and Argentina. Forty accumulated rainwater samples were collected in 30 mL polyethylene bottles in the 2017–2021 period. All these samples were analysed for $\delta^{18}O$ and δ^2H at the University of Waterloo-Environmental Isotope Laboratory (uwEILAB) using a Los Gatos Research Off-Axis Integrated Cavity Output Spectroscopy (LGR-OA-ICOS) laser system. The analytical uncertainty is ±0.2‰ for $\delta^{18}O$ and ±0.8‰ for δ^2H. Precipitation samples were also collected at 24 other sites in the eastern part of the Salar de Atacama during several field trips, capturing precipitation events between January, March and June 2017, and January and March 2019. These rainfall samples were obtained at different elevations through samplers deployed in the study area. These samplers consisted of a screen-covered funnel and collection bottle containing 2.5 cm of vaseline (petroleum jelly) or liquid paraffin to prevent evaporation of the underlying water. The samples were retrieved periodically during the study or as soon after the rain event as was logistically possible. The volume of the water sample was measured and then extracted from each rain catcher with a syringe and transferred to a plastic bottle. Analyses were performed at the Environmental Isotope Laboratory of the University of Arizona. $\delta^{18}O$ and δ^2H were measured on a gas-source isotope ratio mass spectrometer (Finnigan Delta S). Data are reported in ‰ relative to the V-SMOW standard. Hydrogen and oxygen isotope ratios were measured separately. For hydrogen, samples were reacted at 750 °C with Cr metal using a Finnigan H/Device coupled to the mass spectrometer. For oxygen,

samples were equilibrated with CO_2 gas at approximately 15 °C in an automated equilibration device coupled to the mass spectrometer. As waters are isotopically light, a two-point calibration was applied, the international references Vienna Standard Mean Ocean Water (VSMOW) and Standard Light Antarctic Precipitation (SLAP). The precision was 0.9‰ or better for δ^2H and 0.08‰ or better for $\delta^{18}O$ on the basis of repeated internal standards. Additionally, precipitation isotopic data (accumulated samples) from previously published studies carried out in the study area were included in this analysis (Cortecci et al., 2005; CRICYT, 2017; Godfrey et al., 2003; Herrera et al., 2016; Lagos, 2016; Moran et al., 2019). The complete dataset consists of 113 isotope analyses in the 2000–2017 period.

The second group corresponds to surface water samples of rivers, intermittent and permanent streams, ephemeral lagoons, lagoons and lakes. The dataset consists of 158 isotope analyses in the 1994–2019 period in the Salar de Atacama basin (Amphos 21, 2009a; Chaffaut et al., 1998; CRICYT, 2017; Godfrey et al., 2003; Herrera et al., 2019; Moran et al., 2019; Ortiz et al., 2014; SGA, 2015a, 2015b) and 48 isotope analyses in the 1968–2019 period from basins on the Altiplano-Puna Plateau (Cervetto, 2012; Chaffaut et al., 1998; DICTUC, 2009; Herrera et al., 2016, 2019; Lagos, 2016; Moran et al., 2019), as shown in Fig. 2.

The third group contains groundwater samples from wells, piezometers, pits and springs. The Salar de Atacama basin has a halite nucleus (core) whose high porosity is filled by brine in the centre of the basin and a marginal zone resulting from the density contrast between the brine and the freshwater coming from the eastern slope and ranges (Houston, 2006b; IDAEA-CSIC, 2017; Marazuela et al., 2019b). For this reason, wells and piezometers in the salt flat that are affected by the core salt have been excluded, that is, the entire core up to the marginal zone or middle mixing zone (Marazuela et al., 2018). The depth of the wells and piezometers varies between 1 m and 280 m. The dataset of analytical results of samples from the Salar de Atacama periphery that are not affected by the core salts consists of 404 water isotope analyses in the 1994–2019 period (Amphos 21, 2009b; Chaffaut, 1998; CRICYT, 2017; Fock, 2009; Godfrey et al., 2003; Huerta Vásquez, 2012; Moran et al., 2019; Ortiz et al., 2014; Rissmann et al., 2015; SGA, 2015b; Tassi et al., 2010). There are 275 isotope analyses in the 1994-2015 period from basins on the Altiplano-Puna Plateau (Cervetto, 2012; Chaffaut, 1998; Chaffaut et al., 1998; DICTUC, 2009; Herrera et al., 2016; Lagos, 2016; Moran et al., 2019; Risacher et al., 1999).

The deuterium excess (d-ex), defined by d-ex $= \delta^2H - 8\delta^{18}O$ (Dansgaard, 1964), and the evaporation line (EL) as a regression line through the water isotope data of each subbasin are calculated. EL intercepts with the Global Meteoric Water Line (GMWL) points out the original water reservoir impacted by isotopic fractionation processes. The GMWL considered here is $\delta^2H = 8\delta^{18}O + 10‰$, which is accurate enough for the calculations and comparisons.

4. Results

4.1. Meteorology and sea surface temperature

The meteorological parameters present a clear seasonal cycle (Fig. 3). The maximum values of temperature (Fig. 3. A.1), relative humidity (Fig. 3. B.1) and precipitation (Fig. 3. C.1) occur in summer, while the minimum values occur in winter.

The air temperature decreases with elevation, with a temperature gradient of −0.62 °C per 100 m (Fig. 3. A.2). January and February are the warmest months of the year: the average temperature is 19.9 °C and 19.6 °C, the minimum temperature is 16 °C and 16.7 °C, and the maximum temperature is 22.6 °C and 22.4 °C, respectively, between 2300 m asl and 2500 m asl, decreasing to an average temperature of 4.5 °C and 4.8 °C, a minimum temperature of −4.3 °C and −0.3 °C and a maximum temperature of 12.8 °C and 7,7 °C, respectively, above 4000 m asl. June and July are the coldest months of the year: the average temperature is 9.2 °C and 9.1 °C, the minimum is 5.8 °C and 5.6 °C and the maximum
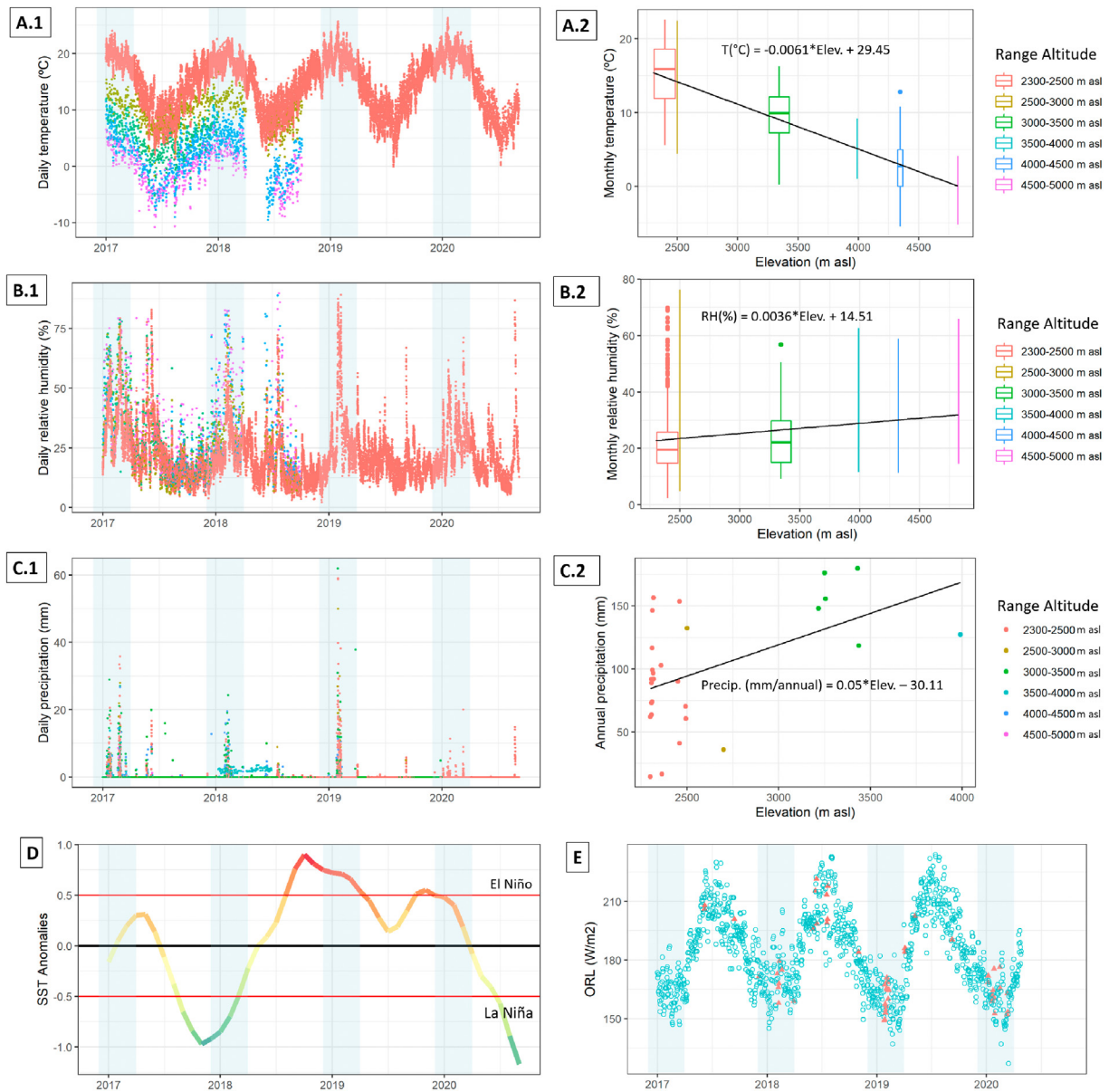
Fig. 3. Meteorological variables A.1) temporal evolution of daily temperature, A.2) temperature altitudinal gradient; B.1) temporal evolution of daily relative humidity; B.2) relative humidity altitudinal gradient; C.1) temporal evolution of daily precipitation; C.2) annual precipitation altitudinal gradient; D) temporal evolution of sea surface temperatures (SST) anomalies, and E) temporal evolution of non-interpolated OLR values: the blue circles are values in the Salar de Atacama basin between 2017 and 2020 and pink triangles are values of the outgoing longwave radiation (OLR) the day in which isotopic samples were collected in the PALMEX passive precipitation samplers in the Salar de Atacama basin.

temperature is 14.9 °C and 12.6 °C, respectively, between 2300 and 2500 m asl, decreasing to an average temperature of −1.2 °C and −1.6 °C, a minimum temperature of −5.2 °C and −5.5 °C and a maximum temperature of 3.0 °C and 2.7 °C, respectively, above 4000 m asl (Fig. SM 2). The temperature is below zero in May, June, July and August above 4000 m asl and in September and October over 4500 m asl.

The relative humidity increases with elevation, with a gradient of 0.36% per 100 m (Fig. 3. B.2). At altitudes between 2500 m asl and 3000 m asl, there was a 10-15% increase in relative humidity in all months, and between 3000 m asl and 3500 m asl there was a similar decrease. February is the month with the highest humidity of the year: the average relative humidity is 35%, the minimum relative humidity is 15.7%, and the maximum relative humidity is 69.8% between 2300 m asl and 2500 m asl, increasing to 50% above 4500 m asl. September and October have the lowest air humidity of the year: the average humidity is 14% and 14.3%, the minimum humidity is 7.3% and 6.1%, and the maximum humidity is 34.3% and 34.2% between 2300 m asl and

2500 m asl, increasing to an average humidity of 19.6% and 18.5%, a minimum humidity of 17.7% and 14.6%, and a maximum humidity of 22.8% and 24.4% over 4500 m asl.

Precipitation increases with elevation, with a gradient of 5 mm/year per 100 m, similar to the 4.6-5.0 mm per 100 m in the literature (IDAEA-CSIC, 2017; Salas et al., 2010). January and February are the rainiest months of the year, with 18.5 mm/month and 34 mm/month respectively, with a decrease to 3 mm/month in March. The rest of the months have extremely dry average values (<1 mm/month), except May (2 mm/month), June (4 mm/month), July (1.3 mm/month) and August (1.9 mm/month).

El Niño/La Niña is a phenomenon in the equatorial Pacific Ocean that is characterized by five consecutive sea surface temperature (SST) anomalies during three consecutive months (https://www.ncdc.noaa. gov/teleconnections/enso/indicators/sst/). Warm (El Niño) and cold (La Niña) periods were based on a threshold of ±0.5 °C for the Oceanic Niño Index (ONI) (Fig. 3D). This standard measurement is known as the Oceanic Niño Index (ONI 3.4) (Center National Weather Service/Climate

Prediction, 2021). It is important to mention that not all altitude ranges have registered months affected by these events. At low altitudes (below 3000 m asl), the summers affected by La Niña are the hottest (Supplementary Material, Fig. SM3) and the driest (Andressen et al., 2007), and if they are affected by El Niño, they are rainier (Supplementary Material, Fig. SM7). The coldest winters at low altitudes (below 3000 m asl) are affected by La Niña and at high altitudes they are the neutral (normal) years. Between 2300 and 2500 m asl, all neutral months are more humid except February, March and April, which are affected by La Niña. Between 2500 and 3000 m asl, from July to December, the months affected by La Niña are the least humid, while those affected by El Niño are the most humid (Supplementary Material, Fig. SM5).

4.2. Precipitation and air mass trajectories

The HYSPLIT model (Stein et al., 2015) was used to identify the preferential transport pathways followed by the air masses that arrived at a point where a rain sample was obtained. It was found that for a given day, the back trajectories are similar for 1500, 3000, 5500 m AGL (above ground level) at the coordinates of the Chaxa and LZA3-1 rain samplers on the days that rain was recorded (the results are available as Supplementary Material, SM_HYSPLIT). The following results are based on the back trajectories at 1500 m AGL.

During the austral summer months (December (Fig. 4C), January (Fig. 4A), February (Fig. 4B) and March (Fig. 4C)), the daily back trajectories were classified into three groups. The first group of trajectories, corresponding to the trade winds, drag very humid air masses from the North Atlantic Ocean across the Amazon basin towards the southwest. They comprise 32% of the trajectories (8 trajectories, average precipitation is 4.2 mm) in Chaxa and 50% (11 trajectories, average precipitation is 6.2 mm) in LZA3-1 (Aravena et al., 1989; Garreaud et al., 2003; Garreaud, 1999, 2000; Lowenstein et al., 2003; Vuille, 1999). The second group consists of continental paths transporting moisture from the South Atlantic Ocean (40% of the paths, 10 trajectories, average precipitation is 4.5 mm, in Chaxa and 26%, 6 trajectories, average precipitation is 2.8 mm, in LZA1-3) and across the La Plata River basin and the Gran Chaco (Insel et al., 2009; Marengo et al., 2002; Pabón-Caicedo et al., 2020; Rasmussen and Houze, 2016; Saulo et al., 2000; Silva et al., 2010). The third group consists of trajectories of moisture masses that come from the Pacific Ocean: 28% of the trajectories (5 trajectories, average precipitation is 3.5 mm) in Chaxa and 26% (3 trajectories, average precipitation is 0.8 mm) in LZA3-1. All the trajectories that were carried out in January, February, March 2019 and 2020 are affected by El Niño and February 2018 trajectories were affected by La Niña. During the austral winter and autumn months (Fig. 4D) all air masses come from the Pacific Ocean 100% of the trajectories (10 trajectories, average precipitation is 1.6 mm, in Chaxa and 11 trajectories, average precipitation is 3.2 mm, in LZA3-1) (Aravena et al., 1999; Fuenzalida and Rutllant, 1986; Garreaud et al., 2003; Valdivielso et al., 2020; Vuille, 1999). However, some months are affected by El Niño (3 of the trajectories in Chaxa and LZA3-1), La Niña (2 of the trajectories in LZA3-1) and neutral (normal) years (7 and 6 of the trajectories in Chaxa and LZA3-1, respectively).

Therefore, more abundant precipitation occurs in summer than in winter. And in summer, air masses from the Atlantic Ocean produce more precipitation than air masses from the Pacific Ocean. However, there are differences in quantity between the Chaxa station (north of the Salar) and the LZA3-1 station (east of the Salar).

4.3. Convective activities

The OLR (outgoing longwave radiation) values also have a marked seasonal cycle characterized by minimum values during the summer months and maximum values during the winter months (Fig. 3E). In summer, the OLR decreases to 150 W/m^2, and in winter, the opposite occurs, increasing to 230 W/m^2.

Understanding the spatial and temporal variations in OLR is important to determine the dynamics of the water balance at various scales, as the OLR depends on the amount of clouds, convective intensity, height of clouds, temperature of the atmosphere and amount of rain (Lim et al., 2013; Morales et al., 2018; Risi et al., 2008a, 2008b). This understanding is important for the management and planning of water resources. The low OLR values of the summer correspond to a greater cloud cover (Fiorella et al., 2015) and to cold and high clouds in the atmosphere, which denotes deep convection (Guo et al., 2017; Vimeux et al., 2011; Vuille et al., 2003, 2008). This deep convective activity originates from the atmospheric circulation that occurs over the Altiplano and the Amazon (Valdivielso et al., 2020) (Fig. 4). The high OLR values of the winter indicate low-level cloudiness or small water vapour content (Vuille et al., 2008). The variation in the amount of seasonal precipitation, which is greater in summer than in winter, is reflected in the OLR values and the precipitation recorded in the rain gauges of the meteorological stations. Therefore, the seasonal cyclicality of the OLR is also not affected by El Niño and La Niña.

4.4. Isotopic composition of precipitation

The 113 precipitation samples (rainfall and snow) considered in this study have a heterogeneous distribution in time and space, with the largest number of samples in the summer and collected between 2300 m asl and 2500 m asl (Table 1).

The linear regression line of the accumulated precipitation samples defined the local meteoric water line (LMWL), expressed by the equation $\delta^2H = 6.9*\delta^{18}O + 1.9$ (Fig. 5C). There is an altitudinal gradient of $\delta^{18}O$ in precipitation samples of −0.15‰ per 100 m, with a coefficient of determination of 0.1 (Fig. 5D); due to this great dispersion of the data, the isotopic composition of precipitation in the Salar de Atacama basin and the Altiplano-Puna Plateau basins was characterized by averaging the stable isotope content values by elevation ranges (Fig. 5A). Average precipitation shows a progressive depletion of heavy isotopes as elevation increases, except for an enrichment in heavy isotopes in the range of 4000–4500 m asl with respect to the isotopic composition in the lower elevation range. This exception may be related to the high standard deviation caused by the high dispersion of the samples. The average deuterium excess is 8.9‰, and it increases progressively from 4.7‰ in the range of 2300–2500 m asl to 16‰ in the range of 4500–5000 m asl (Fig. 5D). In January and February, the average deuterium excess is 7.7‰, and it increases to 13.5‰ in May, June and July.

This isotopic evolution of precipitation is consistent with the temperature and altitude effects. The temperature is lower at higher altitudes, which causes a greater isotopic fractionation effect in the condensation of the vapour, producing precipitation that is richer in heavy isotopes at low altitudes and progressively lighter precipitation as the vapour rises in altitude. This altitudinal gradient calculated for precipitation (-0.15‰ per 100 m) is in the lower range of found values (between −0.15‰ and −0.5‰ per 100 m) (Clark and Fritz, 1997), and it is smaller than some of the $\delta^{18}O$ altitudinal gradients obtained in northern Chile, 0.2‰ per 100 m (Aravena et al., 1989) and −0.5‰ per 100 m (DICTUC, 2008). The $\delta^{18}O$ isotopic gradient determined in the Collacagua area is approximately −0.2‰ per 100 m (Acosta and Custodio, 2008); in the Loa Alto area, it is −0.26‰ per 100 m (Villablanca, 2009); and in the Tuyajto lagoon, it is −0.34‰ per 100 m (Herrera et al., 2016).

In the previous sections, it was observed that there is a clear seasonal difference in meteorological parameters and in the origin and type of air masses. For this reason, to analyse the seasonal variation in the isotopic composition of precipitation, the samples were classified into two groups: summer (December-April) and winter (May to November). In general, seasonal variations occur in isotopic composition: rainfall is lighter in winter ($\delta^{18}O‰$ between -8‰ and -14‰) than in summer ($\delta^{18}O‰$ between −4‰ and −11‰) (Fig. 5B). In summer, precipitation is more enriched in heavy isotopes at low elevations and depleted with
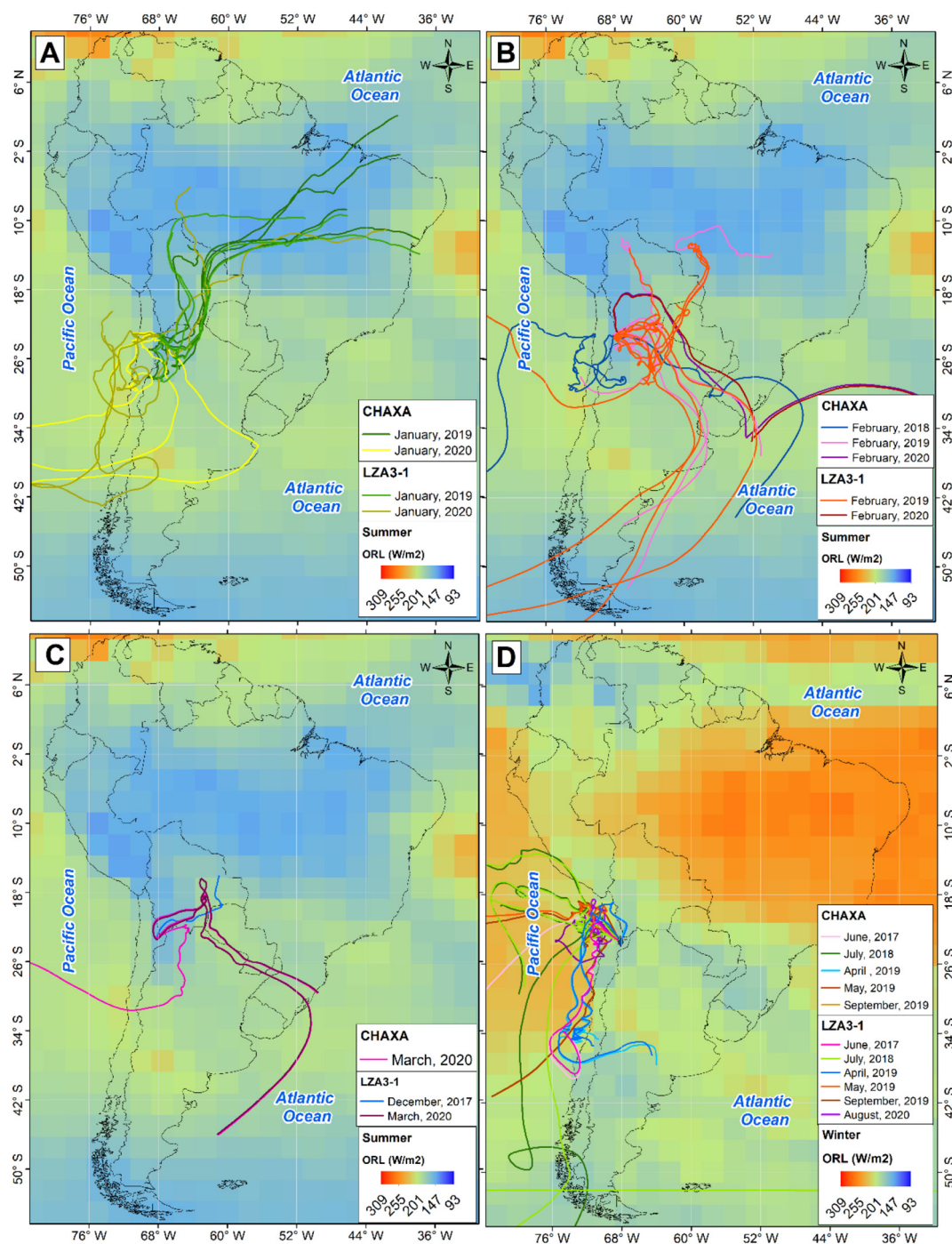
Fig. 4. Back-trajectories indicating potential moisture sources of precipitation (plotted only for days in which precipitation was produced) in Chaxa and LZA3-1. A) January trajectories, B) February trajectories, C) March and December trajectories; average values of the summer months of non-interpolated OLR. D) During the winter (LZA3-1 light green lines and Chaxa dark green lines) and in autumn (LZA3-1); average values of the winter months of non-interpolated OLR.

Table 1
Altitudinal distribution of the number of isotopic accumulated precipitation samples in each of the indicated periods.

Range altitude (m asl)	In the year	In summer	In winter
2300–2500	44	23	15
2500–3000	15	9	5
3000–3500	5	3	2
3500–4000	15	8	5
4000–4500	20	14	5
4500–5000	14	11	2
Total samples	113	68	34

increasing elevation. The linear regression line of the accumulated summer precipitation samples defining the LMWL is expressed by the equation $\delta^2 H = 6.6 * \delta^{18}O + 1$ (Fig. 5E). The altitudinal gradient of $\delta^{18}O$ in summer precipitation samples is −0.21‰ per 100 m, with a coefficient of determination of 0.2. Deuterium excess increases from 2.9‰ in the range of 2300–2500 m asl up to 20‰ in the range of 4500–5000 m asl (Fig. 5F). In winter, precipitation is more enriched in heavy isotopes at low elevations and lighter with increasing elevation up to 3000–3500 m asl, but it becomes more enriched (heavier) again at higher elevations. It is important to note the low number of winter samples (2 or 5 samples per 500 m elevation) above 2500 m asl
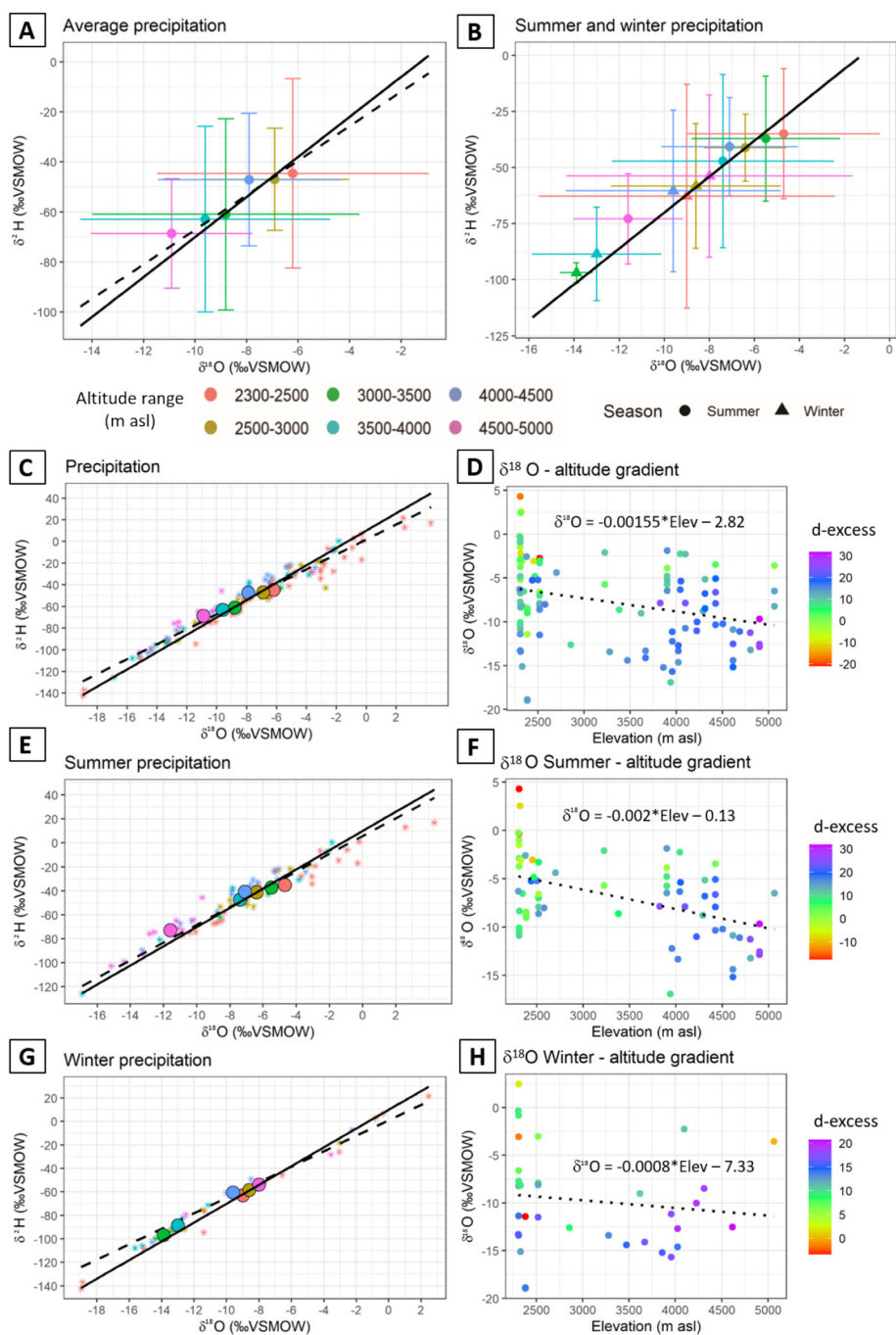
Fig. 5. Isotopic composition of precipitation. A) Average values of $\delta^{18}O$ and $\delta^{2}H$ and its standard deviation of precipitation data by altitude range. The black line is the GMWL B) Average values of summer precipitation (circles) and winter precipitation (triangles). C) The values of precipitation and average values of $\delta^{18}O$ and $\delta^{2}H$. D) $\delta^{18}O$ - altitude for precipitation; the colour indicates values of deuterium excess. E) Values of summer precipitation and average values of summer precipitation. F) $\delta^{18}O$ of summer precipitation - altitude relationships. G) The values of winter precipitation and average values of winter precipitation. H) $\delta^{18}O$ of winter precipitation - altitude relationships.

(Table 1). The linear regression line of the accumulated winter precipitation samples defining the LMWL is expressed by the equation $\delta^{2}H = 7.4 * \delta^{18}O + 5.8$ (Fig. 5G). The altitudinal gradient of $\delta^{18}O$ in winter precipitation samples is $-0.08‰$ per 100 m, with a coefficient of determination of 0.02. Deuterium excess increases progressively from 9.1‰ to 16.5‰ from 4000 to 4500 m asl (Fig. 5H), with the highest value corresponding to unaltered precipitation.

4.5. Surface water and groundwater isotopic compositions

The water isotopic data are plotted in the $\delta^{2}H$-$\delta^{18}O$ diagram of Fig. 6, distinguishing between groundwater (Fig. 6A, A.1, A.2, A.3) and surface water (Fig. 6B, B.1, B.2, B.3). Springs may be in one or the other group, depending on whether the sample is taken at the spring itself or corresponds to flowing water in a stream fed by a spring. The isotopic composition of both surface and groundwater indicates that they are affected by evaporation. The surface water in a given sub-basin has an isotopic composition similar to that of groundwater in the sub-basin, in both the Salar de Atacama and the Altiplano-Puna Plateau (Table 2). The surface water and groundwater of the Altiplano-Puna Plateau basins are isotopically lighter than the surface water and groundwater of the Salar de Atacama sub-basins. In the study area, the waters in northern Altiplano are the most depleted (lighter) in heavy isotopes, followed by those in southern Altiplano.
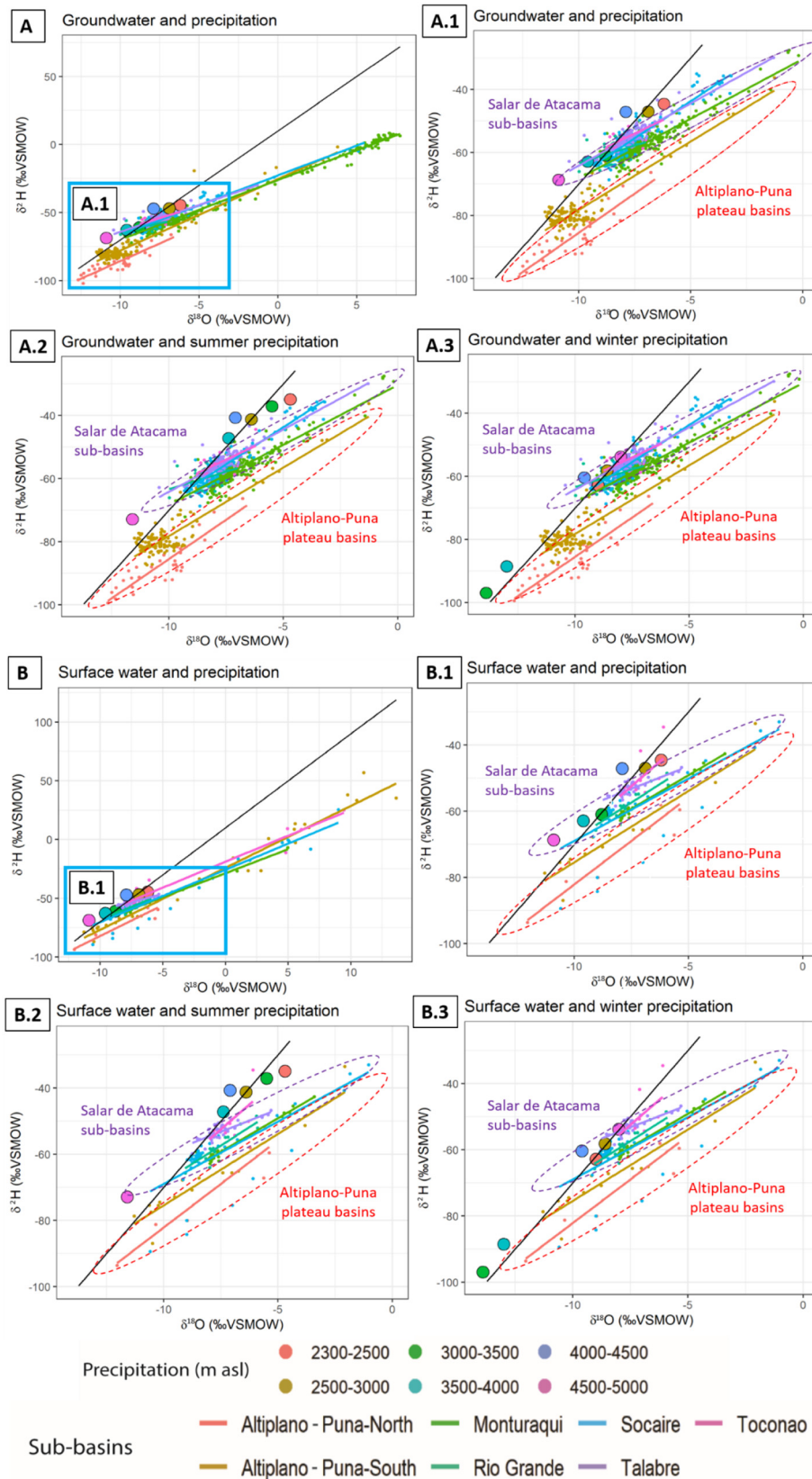
Fig. 6. A) Average values of δ^{18}O and δ^{2}H of annual precipitation by altitude range and groundwater by sub-basins. A.1) Detail of graph A.1. A.2) Detail of the average values of δ^{18}O and δ^{2}H of summer precipitation by altitude range and groundwater by sub-basins. A.2) Detail of the average values of δ^{18}O and δ^{2}H of winter precipitation by altitude range and groundwater by sub-basins. B) The average values of δ^{18}O and δ^{2}H of annual precipitation by altitude range and surface water by sub-basins. B.1) Detail of graph B.1. B.2) Detail of the average values of δ^{18}O and δ^{2}H of summer precipitation by altitude range and surface water by sub-basins. B.3) Detail of the average values of δ^{18}O and δ^{2}H of winter precipitation by altitude range and surface water by sub-basins. The black line is the GMWL.

Table 2
Evaporation line (EL) of each sub-basin and type of water and value of δ²H‰ and δ¹⁸O‰ when the EL intersects in each sub-basin. R² is the coefficient of determination.

Sub-basin	Groundwater				Surface water			
	Evaporation line	R²	δ²H‰	δ¹⁸O‰	Evaporation line	R²	δ²H ‰	δ¹⁸O‰
North Altiplano-Puna plateau	$\delta^2H‰ = 5.2*\delta^{18}O‰ - 33.8$	0.80	−114	−15.5	$\delta^2H‰ = 5.3*\delta^{18}O‰ - 29.5$	0.88	−105	−14.4
South Altiplano-Puna plateau	$\delta^2H‰ = 5.2*\delta^{18}O‰ - 25.4$	0.87	−92	−12.8	$\delta^2H‰ = 5.3*\delta^{18}O‰ - 24.1$	0.97	−90	−12.5
Monturaqui	$\delta^2H‰ = 4.4*\delta^{18}O‰ - 26$	0.98	−69	−10	$\delta^2H‰ = 4.1*\delta^{18}O‰ - 28.6$	0.99	−72	−10
Socaire	$\delta^2H‰ = 4.4*\delta^{18}O‰ - 22.7$	0.90	−62	−9	$\delta^2H‰ = 4.5*\delta^{18}O‰ - 25.7$	0.91	−70	−10
Talabre	$\delta^2H‰ = 4*\delta^{18}O‰ - 24.7$	0.75	−58	−8.5	$\delta^2H‰ = 2.7*\delta^{18}O‰ - 32.9$	0.58	−55	−8.1
Toconao	$\delta^2H‰ = 3.4*\delta^{18}O‰ - 28.6$	0.40	−57	−8.4	$\delta^2H‰ = 4.4*\delta^{18}O‰ - 18.8$	0.96	−54	−8.1
Río Grande	$\delta^2H‰ = 2.2*\delta^{18}O‰ - 41.1$	0.13	−61	−8.8	$\delta^2H‰ = 4.4*\delta^{18}O‰ - 24.2$	0.80	−66	−9.5

The water evaporation lines of the North and South Altiplano-Puna Plateau subbasins, with a slope of approximately 5.2 (Table 2), intersect the GMWL between $\delta^2H = -113‰$ and $-92‰$ for groundwater and between −106‰ and −90‰ for surface water. The waters of the subbasins of the Salar de Atacama are isotopically heavier. Evaporation lines intersecting the GMWL are defined as being between −69‰ and −58‰ δ^2H for groundwater and between −72‰ and −55‰ δ^2H for surface water. The coefficients of determination of the linear regression of groundwater in the Toconao and Río Grande subbasins are low, 0.4 and 0.13, respectively, because the samples are not aligned and cluster close to the GMWL.

Therefore, the meteoric waters that supply the waters of the highlands are lighter than the meteoric waters recharging the basins of the Atacama salt flat. In addition, there is a progressive enrichment in heavy isotopes from the southern subbasins to the northern subbasins (following the sequence Monturaqui, Socaire, Talabre and Toconao), with the exception of the Río Grande sub-basin in the northern part of the Salar de Atacama basin.

5. Discussion

As described in the previous section, there are meteorological differences in the origin of the air masses and the type of clouds that produce precipitation in summer and in winter (Fig. 4), which explain the seasonal variation in the isotopic composition of precipitation (Fig. 5B). For example, summer precipitation results from the air humidity of atmospheric masses with a longer path across the continent than winter precipitation; therefore, summer precipitation should be more depleted in heavy isotopes, although it incorporates more recycled vapour due to evaporation in the continent from free water in surface water bodies and wetlands, which is isotopically heavier. Additionally, according to Risi et al. (2008a), when convection is more intense (in summer), the convective air mass flows are stronger and reach higher levels, and the related unsaturated air downdrafts are enhanced. Therefore, the sub-cloud vapour is more depleted in heavy isotopes than the vapour produced by the less intense winter convection activity. It seems that these effects do not dominantly affect the precipitation in the Salar de Atacama. The observed enrichment of summer precipitation in heavy isotopes and low deuterium excess is probably caused by partial evaporation of raindrops during rainfall. Therefore, the deuterium excess of precipitation is smaller on the ground than at the cloud base. The three groups of air mass trajectories that cause precipitation in summer cannot be isotopically differentiated because the samples analysed are accumulated samples from several different precipitation events. However, depletion of winter precipitation in heavy isotopes and the high values of the deuterium excess derive from precipitation originating in vapour re-evaporated from the soil (Putman et al., 2019).

The surface water evaporated in a given subbasin has an isotopic composition similar to that of groundwater in the subbasin in both the Salar de Atacama and the Altiplano-Puna Plateau. Therefore, recharge is derived from the infiltration of surface waters evaporated from lakes, rivers, wetlands and river channels (Jasechko, 2019). The analysis of the relationship between surface water and groundwater has been carried out in subbasins to determine if there is local or regional recharge from the highlands to the Atacama salt flat. The groundwater of the wells and piezometers of the Salar de Atacama peripheral aquifers considered here is not affected by the nucleus because their plots are aligned in the evaporation line with the shallow groundwater (Fig. 6A).

The precipitation falling between 3000 and 5000 m asl fits the isotopic composition (before fractioning processes due to evaporation) of both groundwater (Fig. 6. A1) and surface water (Fig. 6. B1) in the eastern subbasins of the Salar de Atacama. In the Altiplano-Puna Plateau basins, surface water and groundwater correspond to lighter precipitation than that sampled in this study, which is consistent because the floor areas of the Altiplano-Puna Plateau basins are more than 4000 m asl and are surrounded by volcanoes which top exceeds 6000 m asl, so they receive precipitation from higher altitudes than the precipitation analysed in this study (Fig. 6).

The relationship between seasonal variation in rainfall and the isotopic footprint of surface and groundwater has not been clearly identified. Winter precipitation is more similar to meteoric waters that originate from surface and underground waters. However, this differentiation cannot be made because groundwater samples are a mixture of recharge waters of different altitudes and with variable flow times. Moran et al. (2019) obtained similar isotopic compositions of what they called "premodern" (>60 years old) groundwater, based on the tritium content. However, Godfrey et al. (2003) identified that the meteoric water sources for the Salar de Atacama and Altiplano basins are the same and modern, discarding paleoclimate effects. Groundwater apparent ages over 60 years old are compatible with the existence of modern recharge due to the long transit times through the often very thick unsaturated zone and long way in the aquifers.

This isotopic difference between the waters of the Altiplano - Puna Plateau basins and the Salar de Atacama and the isotopic similarity of rainfall and the waters of the Salar de Atacama support the hypothesis that recharge to the eastern peripheral alluvial aquifers of the Salar de Atacama is due to local precipitation and surface water generated within the hydrographic basin. Focused mechanisms can be triggered by storm events in fractured lavas and gullies, and infiltrate downstream in alluvial fans. The studies that consider that there is a water imbalance between recharge by rainfall and evapotranspiration in the Salar de Atacama basin and, therefore, that there is an additional contribution of groundwater from the Altiplano-Puna Plateau basins (Boutt et al., 2021; Corenthal et al., 2016; Moran et al., 2019; Salas et al., 2010) probably underestimate the recharge mechanisms and rates. They consider that there is no diffuse recharge when precipitation is less than 120 mm (Houston, 2009) and do not take into account snowmelt contributions (50–80 mm/year of snow water equivalent), of which 20%–30% sublimates or is exported by wind before infiltrating (Moran et al., 2019). In the Tuyajto basin, east of the Salar de Atacama, Urrutia et al. (2019) found through an energy balance that snow apparently does not contribute much to groundwater recharge, as snow falling in the lower parts of the basins sublimates in a short time. The DGA stations that measure snowfall in the Altiplano basins east of the Salar de Atacama have discontinuous and unreliable snowfall records. The DGA (2013) study, based on Mardones (1986) and DGA/GCF

(2010), underestimates aquifer hydraulic parameters or overestimates evaporation.

The study area is an example of mountain block recharge (Espinosa et al., 2014; Figueroa et al., 2021; Taucare et al., 2020; Urrutia et al., 2021; Viguier et al., 2019). Mountain-block recharge is composed of mountain block, basin fill and mountain front. A mountain block is an area of topographically elevated and rugged terrain where the shallow subsurface is composed predominantly of bedrock. A mountain block is thus topographically and geologically distinct from adjacent lowland areas, which are relatively flat and underlain by thick unconsolidated to semi-consolidated sediments ("basin fill") that often form highly productive aquifers. The geologic contact between the mountain block and the adjacent basin fill is the mountain front (HIRAVOL, 2020; Markovich et al., 2019; RAEMIA, 2019; Wilson and Guan, 2004).

In Altiplano, there are numerous salt flats that are probably fed by aquifer recharge and the internal runoff. This possibility is currently being studied, aiming to quantify the water budget with the help of atmospheric chloride deposition if the available data allow for it with a reasonable uncertainty.

6. Conclusions

In the Salar de Atacama and the Altiplano basins adjacent to it, the meteorological parameters (temperature, relative humidity and precipitation), the origin and type of precipitation and the isotopic composition of that precipitation vary seasonally. The maximum values of temperature, relative humidity and precipitation are registered in summer. These abundant precipitations come from 3 different trajectories of air masses: (1) being dragged from the Atlantic Ocean by the Amazon basin; (2) crawling from the South Atlantic Ocean through the La Plata River basin and the Gran Chaco; and (3) crawling and from the Pacific Ocean. The analysis of the summer trajectories was carried out in in January, February, March 2019 and 2020 are affected by El Niño and February 2018 trajectories are affected by La Niña. These precipitations are of the deep convective type, are enriched in heavy isotopes compared to winter precipitations and with lower deuterium excess. Therefore, convective activity and the continental effect do not affect the isotopic composition as much as expected. The recycling effect of vapour from bodies of water and vegetation, and the partial evaporation of raindrops during rainfall have greater implications.

In winter, there are minimum values of temperature and relative humidity, and precipitation is scarce. All the daily rear trajectories of the air masses analysed originate in the Pacific Ocean, which correspond to months affected by El Niño, La Niña and neutral (normal). These precipitations are not due to deep convection, are lighter in heavy isotopes, and have higher deuterium excess than summer precipitations. This isotopic composition is probably due to the low temperatures and the contribution of re-evaporated vapour from the soil.

In the Salar de Atacama basin and the Altiplano-Puna Plateau basins, precipitation shows a progressive depletion of heavy isotopes with increasing elevation. The isotopic composition of evaporated surface water is similar to that of groundwater, demonstrating the infiltration of surface water into the aquifer in each subbasin. The extrapolation of the evaporation lines to characterize the original isotopic composition indicates that there are clear differences between the waters of the Altiplano-Puna Plateau basins and those of the aquifers in the eastern and southern parts of the Salar de Atacama basin. The meteoric source of waters in the Altiplano-Puna Plateau basins is isotopically lighter than waters in the Salar de Atacama basin. Isotopically light water from the Altiplano is not found in the peripheral aquifers of the Salar de Atacama sub-basins, even considering the slope effect (mixing of groundwater recharged at variable elevations along the slope). The meteoric sources of surface water and groundwater in the Salar de Atacama subbasins are consistent with modern rainfall, although a long delay is possible due to the transit time through the unsaturated and saturated zones. For this reason, the isotopic difference identified in this study

between summer and winter rainfall does not show up in surface water and groundwater. This implies that although the rainy season is summer, there is also recharge during winter.

Precipitation at high elevations infiltrates the volcanic cones or produces surface runoff. Therefore, the first volcanic chain of the Chilean Andes (the westernmost volcanoes of the Andes, mountain block) is similar to a "water tower", creating a water table divide around the topographic watershed between the Salar de Atacama basin and the Altiplano-Puna Plateau basins, although it is possible that some of the westernmost lagoons have underground outflows to the west. In streams, part of the surface water infiltrates into ignimbrite formations (mountain front), and another part continues to descend in permanent and intermittent streams to alluvial fans (basin fill), where there is focused (concentrated) recharge.

CRediT authorship contribution statement

Declaration of competing interest

The authors declare that they have no known competing financial interests or personal relationships that could have appeared to influence the work reported in this paper.

Acknowledgements

Appendix A. Supplementary data

Supplementary data to this article can be found online at https://doi.org/10.1016/j.scitotenv.2021.150271.

References

Acosta, O., Custodio, E., 2008. Impactos ambientales de las extracciones de agua subterránea en el Salar del Huasco (norte de Chile). Bol. Geol. Min. 119, 33–50.

Amphos 21, 2009a. Actualización del modelo conceptual de Soncor. Estudio geomorfológico e hidrológico de los sectores adyacentes a los cuerpos de agua supericial del sector Soncor. Observaciones de terreno. SQM internal report, p. 58.

Amphos 21, 2009b. Análisis sistemático de la información hidrológica del PSA. SQM internal report, p. 233.

Andressen, R., Monasterio, M., Terceros, L., 2007. Regímenes climáticos del altiplano sur de Bolivia: una región afectada por la desertificación. Rev. Geogr. Venez. 48, 11–32.

Antonio, A., 2018. Isotopic composition of precipitation during strong El Niño – southern oscillation events in the southeast region of Brazil. Hydrol. Process., 2016–2017 https://doi.org/10.1002/hyp.13351.

Aravena, R., Peña, H., Grilli, A., Suzuki, O., Mordeckai, M., 1989. Evolución isotópica de las lluvias y origen de las masas de aire en el Altiplano chileno. IAEA-TECDOC-502c: Isotope Hydrology Investigations in Latin America, pp. 129–142.

Aravena, R., Suzuki, O., Pena, H., Pollastri, A., Fuenzalida, H., Grilli, A., 1999. Isotopic composition and origin of the precipitation in Northern Chile. Appl. Geochem. 14, 411–422. https://doi.org/10.1016/S0883-2927(98)00067-5.

Boutt, D.F., Corenthal, L.G., Moran, B.J., Munk, L.A., Hynek, S.A., 2021. Imbalance in the modern hydrologic budget of topographic catchments along the western slope of the Andes (21–25°S): implications for groundwater recharge assessment. Hydrogeol. J., 985–1007 https://doi.org/10.1007/s10040-021-02309-z.

Boutt, D.F., Hynek, S.A., Munk, L.A., Corenthal, L.G., 2016. Rapid recharge of fresh water to the halite-hosted brine aquifer of Salar de Atacama, Chile. Hydrol. Process. 30, 4720–4740. https://doi.org/10.1002/hyp.10994.

Cabello, M., Orza, J.A.G., Galiano, V., Ruiz, G., 2008. Influence of meteorological input data on backtrajectory cluster analysis -a seven-year study for southeastern Spain. Adv. Sci. Res. 2, 65–70. https://doi.org/10.5194/asr-2-65-2008.

Center for Climate and Resilience Research, 2020. Datos de precipitación [WWW Document]. www.cr2.cl/datos-de-precipitacion/.

Center National Weather Service/Climate Prediction, 2021. https://origin.cpc.ncep.noaa. gov/products/analysis_monitoring/ensostuff/ONI_v5.php [WWW Document].

Cervetto, M., 2012. Caracterización hidrogeológica e hidrogeoquímica de las cuencas: Salar de Aguas Calientes 2, Puntas negras, Laguna Tuyajto, Pampa Colorada, Pampa Las Tecas y Salar El Laco, II región de Chile. University of Chile Thesis to opt for the little of geologist.

Chaffaut, I., 1998. Precipitations d'altitude, eaux souterraines et changements climatiques de l'Altiplano nord-Chilien PhD Thesis of Université Paris Sud U.F.R. Scientifique D´ Orsay.

Chaffaut, I., Coudrain-Ribstein, A., Michelot, J.L., Pouyaud, B., 1998. Précipitation d'altitude du nord-Chili, origine des sources de vapeur et données isotopiques. Bull. l'Institut Français d'Études Andin. 27, 367–384.

New YorkClark, I.D., Fritz, P., 1997. Environmental Isotopes in Hydrogeology.

Corenthal, L.G., Boutt, D.F., Hynek, S.A., Munk, L.A., 2016. Regional groundwater flow and accumulation of a massive evaporite deposit at the margin of the Chilean Altiplano. Geophys. Res. Lett. 43, 8017–8025. https://doi.org/10.1002/2016GL070076.

CORFO- Amphos 21, 2018. Estudio de modelos hidrogeológicos conceptuales integrados para los salares de Atacama, Maricunga y Pedernales.

Cortecci, G., Boschetti, T., Mussi, M., Lameli, C.H., Mucchino, C., Barbieri, M., 2005. New chemical and original isotopic data on waters from El Tatio geothermal field, northern Chile. Geochem. J. 39, 547–571. https://doi.org/10.2343/geochemj.39.547.

CRICYT, 2017. Segundo informe de avance sobre estudios e investigaciones que intentan explicar el estado actual de ejemplares de algarrobo, en una población ubicada en las proximidades del pozo CAMAR 2 de SQM, en el Salar de Atacama, Chile. https://doi. org/10.1079/BJN20041276.

Dansgaard, W., 1964. Stable isotopes in precipitation. Tellus 16, 436–468. https://doi.org/ 10.3402/tellusa.v16i4.8993.

Dapeña, C., Panarello, H.O., 2005. Composición isotópica de la lluvia de Buenos Aires. Su importancia para el estudio de los sistemas hidrológicos pampeanos. Rev. Latino-Americana Hidrogeol. 4, 17–25.

DGA, 2020. Servicios hidrometeorológicos [WWW Document]. www.dga.cl/ servicioshidrometeorologicos/Paginas/default.aspx.

DGA, 2013. Análisis de la oferta hídrica del salar de Atacama. SDT N 339. http:// bibliotecadigital.ciren.cl/handle/123456789/25996 Santiago, Chile.

DGA, 1986. Evaporación desde salares: metodología para evaluar los recursos hídricos renovables. Aplicación en las regiones I y II Santiago, Chile.

DICTUC, 2009. Levantamiento hidrogeológico para el desarrollo de nuevas fuentes de agua en áreas prioritarias de la zona norte de Chile, regiones XV, I, II y III. Parte IV. Hidrogeoquímica e isotopía regional del Altiplano de Chile. http://sad.dga.cl/ ipac20/ipac.jsp?se.

DICTUC, 2008. Levantamiento hidrogeológico para el desarrollo de nuevas fuentes de agua en áreas prioritarias de la zona norte de Chile, regiones XV, I, II y III. Parte VI. Campañas ede muestreo.

dos Santos, V., Gastmans, D., Sánchez-Murillo, R., Felippe Gozzo, L., Vianna Batista, L., Lilla Manzione, R., Martinez, J., 2019. Regional atmospheric dynamics govern interannual and seasonal stable isotope composition in southeastern Brazil. J. Hydrol. 579, 124136. https://doi.org/10.1016/j.jhydrol.2019.124136.

Draxler, R.R., 1999. HYSPLIT4 user's guide. In: NOAA Tech. (Ed.), Air Resources Laboratory. Tech Memo ERL ARL-230.

Draxler, R.R., Hess, G.D., 1997. Descrption of the HYSPLIT_4 Modeling System. In: NOAA Tech. (Ed.), Air Resources Laboratory. Tech Memo ERL ARL-224.

Duvert, C., Stewart, M.K., Cendón, D.I., Raiber, M., 2016. Time series of tritium, stable isotopes and chloride reveal short-term variations in groundwater contribution to a stream. Hydrol. Earth Syst. Sci. 20, 257–277. https://doi.org/10.5194/hess-20-257-2016.

Espinosa, S., Custodio, E., Loaso, C., 2014. Estimación de la recarga media anual de acuíferos: aplicación a la Vall Baixa de l'Ebre., Congreso Ibérico de las aguas subterraneas. In: Gómez-Hernández, J., Rodrigo-Ilarri, J. (Eds.), CIAS 2014. II Congreso Ibérico de las Aguas Subterráneas. Valencia. 2014. Ed. Universitat Politècnica de València, pp. 285–301 ISBN: 978–84–9048–239–1.

Esquivel-Hernández, G., Mosquera, G.M., Sánchez-Murillo, R., Quesada-Román, A., Birkel, C., Crespo, P., Célleri, R., Windhorst, D., Breuer, L., Boll, J., 2019. Moisture transport and seasonal variations in the stable isotopic composition of rainfall in Central American and Andean Páramo during El Niño conditions (2015–2016). Hydrol. Process. 33, 1802–1817. https://doi.org/10.1002/hyp.13438.

Figueroa, R., Viguier, B., Taucare, M., Yáñez, G., Arancibia, G., Sanhueza, J., Daniele, L., 2021. Deciphering groundwater flow-paths in fault-controlled semiarid mountain front zones (Central Chile). Sci. Total Environ. 771. https://doi.org/10.1016/j.scitotenv. 2021.145456.

Fiorella, R.P., Poulsen, C.J., Zolá, R.S.P., Barnes, J.B., Tabor, C.R., Ehlers, T.A., 2015. Spatiotemporal variability of modern precipitation δ18O in the central Andes and implications for paleoclimate and paleoaltimetry estimates. J. Geophys. Res. Atmos. 120, 4630–4656. https://doi.org/10.1002/2014JD022893.

Fock, A., 2009. Estudio del acuífero aluvial del borde este del salar de Atacama, entre quebradas Camar y Socaire, comuna San Pedro de Atacama, II Región de Antofagasta, Chile. Fundación Centro Internacional de Hidrología Subterránea y Universitat Politècnica de Catalunya, Barcelona.

Fuenzalida, H., Rutllant, J., 1986. Estudio sobre el origen del vapor de agua que precipita en el invierno altiplánico. http://www.dgf.uchile.cl/rene/PUBS/OTHERS/Aceituno_ 96.pdf.

Garreaud, R., Vuille, M., Clement, A.C., 2003. The climate of the altiplano: observed current conditions and mechanisms of past changes. Palaeogeogr. Palaeoclimatol. Palaeoecol. 194, 5–22. https://doi.org/10.1016/S0031-0182(03)00269-4.

Garreaud, R.D., 2000. Intraseasonal variability of moisture and rainfall over the South American Altiplano. Mon. Weather Rev. 128, 3337–3346. https://doi.org/10.1175/ 1520-0493(2000)128<3337:IVOMAR>2.0.CO;2.

Garreaud, R.D., 1999. Multiscale analysis of the summertime precipitation over the Central Andes. Am. Meteorol. Soc. 127 (5), 901–921. https://doi.org/10.1175/1520-0493(1999)127%3C0901:MAOTSP%3E2.0.CO;2.

GCF Ingenieros - DGA, 2010. Actualización de la evaluación de la disponibilidad de recursos hídricos para constituir derechos de aprovechamiento en las subcuencas afluentes al salar de Atacama, II Región. https://doi.org/10.1243/09544100JAERO33.

Godfrey, L.V., Jordan, T.E., Lowenstein, T.K., Alonso, R.L., 2003. Stable isotope constraints on the transport of water to the Andes between 22° and 26°S during the last glacial cycle. Palaeogeogr. Palaeoclimatol. Palaeoecol. 194, 299–317. https://doi.org/10. 1016/S0031-0182(03)00283-9.

González, M., Dapeña, C., Cerne, B., Sánchez-Ccoyllo, O., Freitas, S., Silva Dias, P.L., Panarello, H., 2009. Verification of the geographical origin of modeled air-mass trajectories by means of the isotope composition of rainwater during the SALLJEX experiment. Environ. Fluid Mech. 9, 409–425. https://doi.org/10.1007/s10652-009-9121-z.

Gröning, M., Lutz, H.O., Roller-Lutz, Z., Kralik, M., Gourcy, L., Pöltenstein, L., 2012. A simple rain collector preventing water re-evaporation dedicated to δ 18O and δ 2H analysis of cumulative precipitation samples. J. Hydrol. 448–449, 195–200. https://doi.org/10. 1016/j.jhydrol.2012.04.041.

Guo, X., Tian, L., Wen, R., Yu, W., Qu, D., 2017. Controls of precipitation δ18O on the northwestern Tibetan Plateau: a case study at Ngari station. Atmos. Res. 189, 141–151. https://doi.org/10.1016/j.atmosres.2017.02.004.

Herrera, C., Custodio, E., Chong, G., Lambán, L.J., Riquelme, R., Wilke, H., Jódar, J., Urrutia, J., Urqueta, H., Sarmiento, A., Gamboa, C., Lictevout, E., 2016. Groundwater flow in a closed basin with a saline shallow lake in a volcanic area: Laguna Tuyajto, northern Chilean Altiplano of the Andes. Sci. Total Environ. 541, 303–318. https://doi.org/10. 1016/J.SCITOTENV.2015.09.060.

Herrera, C., Urrutia, M.J., Jódar, J., Lambán, L.J., Custodio, E., Gamboa, C., 2019. Hydrogeological research in the tuyajto lake at the flamingo national reserve (Atacama, Chile). Bol. Geol. Min. 130, 789–806. https://doi.org/10.21701/bolgeomin. 130.4.011.

HIRAVOL, 2020. Hidrogeología y recursos de agua subterránea en formaciones e islas volcánicas. (Hydrogeology and groundwater resources in volcanic formations and islands). http://hdl.handle.net/2117/347150 Barcelona.

Houston, J., 2009. A recharge model for high altitude, arid, Andean aquifers. Int. Food Res. J. 24, 318–326 doi:10.1002/hyp.

Houston, J., 2006a. Variability of precipitation in the Atacama Desert: its causes and hydrological impact. Int. J. Climatol. 26, 2181–2198. https://doi.org/10.1002/joc.1359.

Houston, J., 2006b. Evaporation in the Atacama Desert: an empirical study of spatiotemporal variations and their causes. J. Hydrol. 330, 402–412. https://doi.org/10. 1016/j.jhydrol.2006.03.036.

Huerta Vásquez, G., 2012. Evaluation of Chemical Patterns in Brines in the Salar de Atacama, Northern Chile: A Chemical and Isotopic Approach. University of Waterloo Tesis for degree of Master of Science in Earth and Environmental Sciences.

IDAEA-CSIC, 2017. Cuarta actualización del modelo hidrogeológico del Salar de Atacama. SNIFA. https://snia.sma.gob.cl.

Insel, N., Poulsen, C.J., Ehlers, T.A., 2009. Influence of the Andes Mountains on South American moisture transport, convection, and precipitation. Clim. Dyn. 35, 1477–1492. https://doi.org/10.1007/s00382-009-0637-1.

Jasechko, S., 2019. Global isotope hydrogeology—review. Rev. Geophys. 57, 835–965. https://doi.org/10.1029/2018RG000627.

Jordan, T.E., Munoz, N., Hein, M., Lowenstein, T., Godfrey, L., Yu, J., 2002. Active faulting and folding without topographic expression in an evaporite basin, Chiles. Bull. Geol. Soc. Am. 114, 1406–1421. https://doi.org/10.1130/0016-7606(2002)114<1406: AFAFWT>2.0.CO;2.

Lagos, L., 2016. Hidrogeoquímica de fuentes termales en ambientes salinos relacionados con salares en los Andes del norte de Chile. Universidad de Chile Tesis for degree of Master of Sciences mention in geology.

Liebmann, B., 1996. Description of a complete (interpolated) outgoing longwave radiation dataset. Bull. Am. Meteor. Soc. 77, 1275–1277.

Lim, E.S., Das, U., Pan, C.J., Abdullah, K., Wong, C.J., 2013. Investigating variability of outgoing longwave radiation over Peninsular Malaysia using wavelet transform. J. Clim. 26, 3415–3428. https://doi.org/10.1175/JCLI-D-12-00345.1.

Lowenstein, T.K., Hein, M.C., Bobst, A.L., Jordan, T.E., Ku, T.-L., Luo, S., 2003. An assessment of stratigraphic completeness in climate-sensitive closed-basin lake sediments: Salar de Atacama, Chile. J. Sediment. Res. 73, 91–104. https://doi.org/10. 1306/061002730091.

Marazuela, M.A., Vázquez-Suñé, E., Ayora, C., García-Gil, A., 2020. Towards more sustainable brine extraction in salt flats: learning from the Salar de Atacama. Sci. Total Environ. 703, 135605. https://doi.org/10.1016/j.scitotenv.2019.135605.

Marazuela, M.A., Vázquez-Suñé, E., Ayora, C., García-Gil, A., Palma, T., 2019a. The effect of brine pumping on the natural hydrodynamics of the Salar de Atacama: the damping capacity of salt flats. Sci. Total Environ. 654, 1118–1131. https://doi.org/10.1016/j. scitotenv.2018.11.196.

Marazuela, M.A., Vázquez-Suñé, E., Ayora, C., García-Gil, A., Palma, T., 2019b. Hydrodynamics of salt flat basins: the Salar de Atacama example. Sci. Total Environ. 651, 668–683. https://doi.org/10.1016/j.scitotenv.2018.09.190.

Marazuela, M.A., Vázquez-Suñé, E., Custodio, E., Palma, T., García-Gil, A., Ayora, C., 2018. 3D mapping, hydrodynamics and modelling of the freshwater-brine mixing zone in salt flats similar to the Salar de Atacama (Chile). J. Hydrol. 561, 223–235. https://doi.org/10.1016/j.jhydrol.2018.04.010.

Mardones, L, 1998. Estudio de evaporación en el Salar de Atacama.

Mardones, L, 1986. Características geológicas e hidrogeológicas del Salar de Atacama. In: Lagos, G. (Ed.), El Litio, Un Nuevo Recurso Para Chile, pp. 181–216.

Marengo, J.A., Douglas, M.W., Silva Dias, P.L., 2002. The South American low-level jet east of the Andes during the 1999 LBA-TRMM and LBA-WET AMC campaign. J. Geophys. Res. D Atmos. 107. https://doi.org/10.1029/2001JD001188.

Markovich, K.H., Manning, A.H., Condon, L.E., McIntosh, J.C., 2019. Mountain-block recharge: a review of current understanding. Water Resour. Res. 55, 8278–8304. https://doi.org/10.1029/2019WR025676.

Morales, M.S., Christie, D.A., Neukom, R., Rojas, F., Villalba, R., 2018. Variabilidad hidroclimática en el sur del Altiplano: pasado, presente y futuro. La Puna argentina Nat. y Cult. 24, 75–91.

Moran, B.J., Boutt, D.F., Munk, L.A., 2019. Stable and radioisotope systematics reveal fossil water as fundamental characteristic of arid orogenic-scale groundwater systems. Water Resour. Res. 55, 11295–11315. https://doi.org/10.1029/2019WR026386.

Munk, L.A., Boutt, D.F., Hynek, S.A., Moran, B.J., 2018. Hydrogeochemical fluxes and processes contributing to the formation of lithium-enriched brines in a hyperarid continental basin. Chem. Geol. 493, 37–57. https://doi.org/10.1016/j.chemgeo.2018.05.013.

Munk, L.A., Boutt, D.F., Moran, B.J., McKnight, S.V., Jenckes, J., 2021. Hydrogeologic and geochemical distinctions in freshwater-brine systems of an Andean Salar. Geochem. Geophys. Geosyst. 22 https://doi.org/10.1029/2020GC009345.

Ortiz, C., Aravena, R., Briones, E., Suárez, F., Tore, C., Muñoz, J.F., 2014. Sources of surface water for the Soncor ecosystem, Salar de Atacama basin, northern Chile. Hydrol. Sci. J. 59, 336–350. https://doi.org/10.1080/02626667.2013.829231.

Pabón-Caicedo, J.D., Arias, P.A., Carril, A.F., Espinoza, J.C., Borrel, L.F., Goubanova, K., Lavado-Casimiro, W., Masiokas, M., Solman, S., Villalba, R., 2020. Observed and projected hydroclimate changes in the Andes. Front. Earth Sci. 8, 1–29. https://doi.org/10.3389/feart.2020.00061.

Pourrut, P., Covarrubias, A., 1995. Existencia de agua en la II Región de Chile: interrogantes e hipótesis. Bulletin Institut Francais D'Études Andines, pp. 505–515.

Putman, A.L., Fiorella, R.P., Bowen, G.J., Cai, Z., 2019. A global perspective on local meteoric water lines: meta-analytic insight into fundamental controls and practical constraints. Water Resour. Res. 55, 6896–6910. https://doi.org/10.1029/2019wr025181.

RAEMIA, 2019. Recarga natural a los acuíferos, metodología y soporte de la isotopía del agua. Aplicación a la planificación hidrológica y conocimiento de las aguas subterráneas en España. http://hdl.handle.net/2117/182282 Barcelona.

Ramírez, C.F., Gardeweg, M., 1982. Carta geológica de Chile, Hoja Toconao, Vol. 54. 1: 250.000. Servicio Nacional de Geología y Minería.

Rasmussen, K.L., Houze, R.A., 2016. Convective Initiation near the Andes in Subtropical South America. Mon. Weather Rev. https://doi.org/10.1175/MWR-D-15-0058.1.

Risacher, F., Alonso, H., Salazar, C., 1999. Geoquímica de aguas en cuencas cerradas: I, II y III Regiones, Chile. Estudio de cuencas de la I Región. S.I.T.No51. Ministerio de Obras Públicas Santiago, Chile http://bibliotecadigital.ciren.cl/handle/123456789/6369.

Risacher, F., Alonso, H., Salazar, C., 1998. Geoquímica de aguas en cuencas cerradas I, II, y III Regiones, Chile. Síntesis.

Risi, C., Bony, S., Vimeux, F., 2008a. Influence of convective processes on the isotopic composition (δ18O and δD) of precipitation and water vapor in the tropics: 2. Physical interpretation of the amount effect. J. Geophys. Res. Atmos. 113.

Risi, C., Bony, S., Vimeux, F., Descroix, L., Ibrahim, B., Lebreton, E., Mamadou, I., Sultan, B., 2008b. What controls the isotopic composition of the African monsoon precipitation? Insights from event-based precipitation collected during the 2006 AMMA field campaign. Geophys. Res. Lett. 35, 1–6. https://doi.org/10.1029/2008GL035920.

Rissmann, C., Leybourne, M., Benn, C., Christenson, B., 2015. The origin of solutes within the groundwaters of a high Andean aquifer. Chem. Geol. 396, 164–181. https://doi.org/10.1016/j.chemgeo.2014.11.029.

Rubilar, J., Martínez, F., Arriagada, C., Becerra, J., Bascuñán, S., 2018. Structure of the Cordillera de la Sal: a key tectonic element for the Oligocene-Neogene evolution of the Salar de Atacama basin, Central Andes, northern Chile. J. S. Am. Earth Sci. 87, 200–210. https://doi.org/10.1016/j.jsames.2017.11.013.

Saavedra, F.A., Kampf, S.K., Fassnacht, S.R., Sibold, J.S., 2017. A snow climatology of the Andes Mountains from MODIS snow cover data. Int. J. Climatol. 37, 1526–1539. https://doi.org/10.1002/joc.4795.

Saavedra, F.A., Kampt, S.K., Fassnacht, S.R., Sibold, J.S., 2018. Changes in Andes Mountains snow cover from MODIS data 2000–2016. Cryosph. Discuss. 12, 1027–1046. https://doi.org/10.5194/tc-2017-72.

Salas, J., Guimerà, J., Cornellà, O., Aravena, R., Guzmán, E., Tore, C., Von Igel, W., Moreno, R., 2010. Hidrogeología del sistema lagunar del margen este del Salar de Atacama (Chile). Bol. Geol. Min. 121, 357–372.

Sánchez-Murillo, R., Aguirre-Dueñas, E., Gallardo-Amestica, M., Moya-Vega, P., Birkel, C., Esquivel-Hernández, G., Boll, J., 2018. Isotopic characterization of waters across Chile. Andean Hydrology, pp. 205–230 https://doi.org/10.1201/9781315155982-9.

Saulo, A.C., Nicolini, M., Chou, S.C., 2000. Model characterization of the South American low-level flow during the 1997–1998 spring-summer season. Clim. Dyn. 16, 867–881. https://doi.org/10.1007/s003820000085.

SERNAGEOMIN, 2003. Geological Map of Chile: digital version. 1:1,000,000. Publishing, No. 4 (CD-ROM, version 1.0, 2003). www.ipgp.fr/~dechabal/Geol-millon.pdf. (Accessed 2 November 2021).

SGA, 2015a. EIA. Proyecto modificaciones y mejoramiento del sistema de pozas de evaporación solar en el salar de Atacama. Apéndice B. Geofísica.

SGA, 2015b. EIA. Proyecto modificaciones y mejoramiento del sistema de pozas de evaporación solar en el salar de Atacama. Apéndice K. Planillas del Modelo Numérico.

Silva, G.A.M., Ambrizzi, T., Marengo, J.A., 2010. Observational evidences on the modulation of the South American Low Level Jet east of the Andes according the ENSO variability. Ann. Geophys. 27, 645–657. https://doi.org/10.5194/angeo-27-645-2009.

Stein, A.F., Draxler, R.R., Rolph, G.D., Stunder, B.J.B., Cohen, M.D., Ngan, F., 2015. NOAA's HYSPLIT atmospheric transport and dispersion modeling system. Bull. Am. Meteorol. Soc. 96, 2059–2077. https://doi.org/10.1175/BAMS-D-14-00110.1.

Tassi, F., Aguilera, F., Darrah, T., Vaselli, O., Capaccioni, B., Poreda, R.J., Delgado Huertas, A., 2010. Fluid geochemistry of hydrothermal systems in the Arica-Parinacota, Tarapacá and Antofagasta regions (northern Chile). J. Volcanol. Geotherm. Res. 192, 1–15. https://doi.org/10.1016/j.jvolgeores.2010.02.006.

Taucare, M., Daniele, L., Viguier, B., Vallejos, A., Arancibia, G., 2020. Groundwater resources and recharge processes in the Western Andean Front of Central Chile. Sci. Total Environ. 722, 137824. https://doi.org/10.1016/j.scitotenv.2020.137824.

Tejeda, I., Cienfuegos, R., Muñoz, J.F., Durán, M., 2003. Numerical modeling of saline intrusion in Salar de Atacama. J. Hydrol. Eng. 8, 25–34. https://doi.org/10.1061/(ASCE)1084-0699(2003)8:1(25).

Urrutia, J., Guimerà, J., Custodio, E., Herrera, C., Jódar, J., Acosta, O., Ansón, I., 2021. Processes explaining the origin and evolution of groundwater composition in the Andean Precordillera and Altiplano of the Tarapacá Region of northern Chile. Submitted. Sci. Total Environ., 149742 https://doi.org/10.1016/j.scitotenv.2021.149742.

Urrutia, J., Herrera, C., Custodio, E., Jódar, J., Medina, A., 2019. Groundwater recharge and hydrodynamics of a complex volcanic aquifer with a shallow saline lake: Laguna tuyajto, andean cordillera of northern Chile. Sci. Total Environ. 134116. https://doi.org/10.1016/j.scitotenv.2019.134116.

Valdivielso, S., Vázquez-Suñé, E., Custodio, E., 2020. Origin and variability of oxygen and hydrogen isotopic composition of precipitation in the Central Andes: a review. J. Hydrol. 587, 124899. https://doi.org/10.1016/j.jhydrol.2020.124899.

Viguier, B., Daniele, L., Jourde, H., Leonardi, V., Yáñez, G., 2019. Changes in the conceptual model of the Pampa del Tamarugal Aquifer: implications for central depression water resources. J. S. Am. Earth Sci. 94, 102217. https://doi.org/10.1016/j.jsames.2019.102217.

Villablanca, D., 2009. Estudio de la relación isotópica δ18O/δ2H de los manantiales en el sector de las nacientes del Loa, Región de Antofagasta. XII Congr. Geológico Chil, pp. 22–26.

Vimeux, F., Tremoy, G., Risi, C., Gallaire, R., 2011. A strong control of the South American SeeSaw on the intra-seasonal variability of the isotopic composition of precipitation in the Bolivian Andes. Earth Planet. Sci. Lett. 307, 47–58. https://doi.org/10.1016/j.epsl.2011.04.031.

Vuille, M., 1999. Atmospheric circulation over the Bolivian Altiplano during dry and wet periods and extreme phases of the Southern Oscillation. Int. J. Climatol. 19, 1579–1600.

Vuille, M., Ammann, C., 1997. Regional snowfall patterns in the high, arid Andes. Clim. Chang. High Elev. Sites 36, 181–191. https://doi.org/10.1007/978-94-015-8905-5_10.

Vuille, M., Baumgartner, M.F., 1998. Monitoring the regional and temporal variability of winter snowfall in the arid Andes using digital noaa/avhrr data. Geocarto Int. 13, 59–67. https://doi.org/10.1080/10106049809354629.

Vuille, M., Bradley, R., Werner, M., Keimig, F., 1998. 20th century climate change in the tropical Andes: observations and model results. J. Intell. Robot. Syst. Theory Appl. 22, 255–267. https://doi.org/10.1023/A.

Vuille, M., Bradley, R.S., Healy, R., Werner, M., Hardy, D.R., 2003. Modeling δ18O in precipitation over the tropical Americas: 2. Simulation of the stable isotope signal in Andean ice cores. J. Geophys. Res. 108, 4175. https://doi.org/10.1029/2001JD002039.

Vuille, M., Francou, B., Wagnon, P., Juen, I., Kaser, G., Mark, B.G., Bradley, R.S., 2008. Climate change and tropical Andean glaciers: past, present and future. Earth-Sci. Rev. 89, 79–96. https://doi.org/10.1016/j.earscirev.2008.04.002.

Wilson, J.L., Guan, H., 2004. Mountain-block hydrology and mountain-front recharge. In: Phillips, F., Hogan, J., Scanlon, B. (Eds.), Groundwater Recharge in a Desert Environment, The Southwestern United States. AGU, Washington, DC, pp. 113–137 https://doi.org/10.1029/009WSA08.